Organic & Biomolecular Chemistry

Accepted Manuscript

This article can be cited before page numbers have been issued, to do this please use: T. Jia, J. Xiang, J. Wang, P. Guo and J. Yu, *Org. Biomol. Chem.*, 2013, DOI: 10.1039/C3OB40799C.

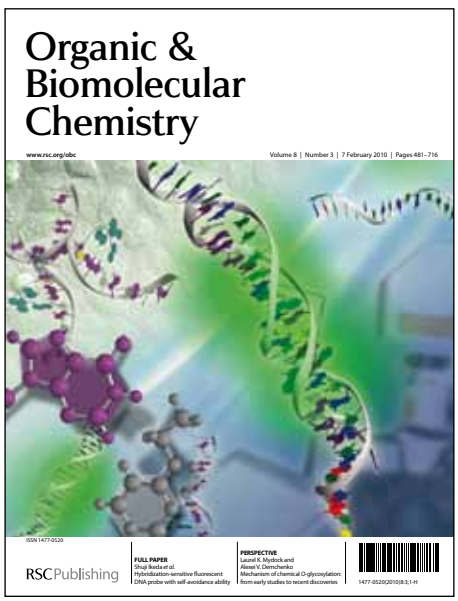

This is an *Accepted Manuscript*, which has been through the RSC Publishing peer review process and has been accepted for publication.

Accepted Manuscripts are published online shortly after acceptance, which is prior to technical editing, formatting and proof reading. This free service from RSC Publishing allows authors to make their results available to the community, in citable form, before publication of the edited article. This *Accepted Manuscript* will be replaced by the edited and formatted *Advance Article* as soon as this is available.

To cite this manuscript please use its permanent Digital Object Identifier (DOI®), which is identical for all formats of publication.

More information about *Accepted Manuscripts* can be found in the **Information for Authors**.

Please note that technical editing may introduce minor changes to the text and/or graphics contained in the manuscript submitted by the author(s) which may alter content, and that the standard **Terms & Conditions** and the **ethical guidelines** that apply to the journal are still applicable. In no event shall the RSC be held responsible for any errors or omissions in these *Accepted Manuscript* manuscripts or any consequences arising from the use of any information contained in them.

DOI: 10.1039/C3OB40799C

Organic & Biomolecular Chemistry

Cite this: DOI: 10.1039/c0xx00000x

ARTICLE TYPE

www.rsc.org/xxxxxx

Interactions of newly designed dicationic carbazole derivatives with double-stranded DNA: syntheses, binding studies and AFM imaging

Tao Jia [a]*, Jin Xiang [a], Jing Wang [b], Peng Guo [a], Junping Yu [b]*

Received (in XXX, XXX) Xth XXXXXXXXX 20XX, Accepted Xth XXXXXXXXX 20XX

DOI: 10.1039/b000000x

The design of small molecular ligands able to bind with DNA is pivotal for development of diagnostic agents and therapeutic drugs targeting DNA. Carbazole-derivatives are potential agents against tumor and opportunistic infections of AIDS. Here, two carbazole-derived dicationic compounds, DPDI and DPPDI, were designed, synthesized and characterized by NMR, IR and MS. The DNA binding properties of DPDI and DPPDI were sensitive to ionic strength. At low ionic strength, planar and aromatic DPDI had a strongly intercalative interaction with DNA, which was confirmed by circular dichroism (CD) and gel electrophoresis. In DPPDI, a phenyl group substituting H atom at –NH group of DPDI destroyed molecular planarity, which resulted in no intercalative interactions between DPPDI and DNA, proved by CD. The positive enhancement of CD at 260-270nm and Hoechst 33258 competitive binding tests indicated the strong groove interactions of both DPPDI and DPDI to DNA. The similarity and difference in the structures between DPDI and DPPDI explained different interaction preferences with DNA. In groove interactions, dications of pyridinium on either DPDI or DPPDI could interact with DNA base pairs, and –NH on DPDI or –N-Ph on DPPDI pointed out of the groove, as the classical model of DNA groove binding agents. Furthermore, AFM imaging revealed that both carbazole-derivatives drove the DNA conformation more compact. All the experimental data proved that the two dicationic carbazole-derivatives interacted with DNA strongly and might act as a novel type of DNA-binding candidate.

Introduction

The interactions between DNA and small molecular ligands are of great importance in biology and medicine, due to their foundational roles in medicinal, biochemical and biological processes. Meanwhile, DNA remains a biological target of major interests for the design of diagnostic agents and therapeutic drugs. Small molecules can interact selectively with DNA by intercalation, or groove binding, but the interaction preferences depend on the structure of DNA-interacting molecules and the nature of DNA. Small differences in the structure of a DNA-interacting molecule may affect the binding types and stability of the molecule/DNA complex [1]. A molecule containing a planar and aromatic moiety is more favorable for intercalation, in which the moiety can slide between the adjacent base pairs and facilitate the intercalation [2, 3]. However, most organic molecules that bind in the DNA grooves have extended conjugated systems with aromatic rings that directly bonded or connected through linking groups such as cationic amidine groups or amidine derivatives (such as DAPI, Hoechst 33258, netropsin) [4-6]. The classical model of DNA groove binding agents is that they have an extended crescent shape that closely fits the helical twist of the groove. [7, 8]

Carbazole derivatives have been reported to be potential agents against tumor [9] or opportunistic infections of AIDS [10, 11]. The carbazoles substituted at 3,6 or 2,7 positions with cationic amidine groups or imidazoline groups have been proved to bind strongly in the DNA groove of AT-rich sequences. [10, 11] These carbazole derivatives look more like classical intercalators with a planar chromophore, so they displayed an intercalating binding mode in GC-rich sequences. [11, 12] For the 3,6-carbazole dicationic derivatives, the geometry is similar to the typical groove ligands having an extended conjugated system with crescent shape. Both terminal cationic amidine groups and imidazoline groups engage H-bonding interactions with the bases while the carbazole –NH points out of the groove. [6-7]

Another type of carbazole-derived cationic compounds (such as BMVC, BHVC), which have extended conjugated systems with carbazoles connected through linking groups to pyridinium, have been successfully used as fluorescent bio-imaging probes with high fluorescence intensity and large two-photon excited fluorescence action cross-sections upon DNA binding. [13-15] The bright fluorescence spots from these carbazole derivatives have been observed in the nuclei of most cancer cells, and hardly found in the nuclei of normal cells. [16] Meanwhile, they can stabilize G-quadruplex DNA structure formed by human telomeric sequence and inhibit telomerase activity. [16-18] However, the binding preferences of these carbazole dications to DNA are not clear.

A carbazole analogue, 5*H*-pyrrolo[3,2-c:4,5-c']dipyridine had a characteristic structure that two C atoms at 3,6-position of carbazole were replaced by two N atoms. [19] Its methylated product, 2,8-dimethyl-5H-pyrrolo[3,2-c:4,5-c']dipyridinium diiodide (**DPDI**, the structure is shown in Fig.1.), has a similar geometry to 3,6-carbazole dicationic derivatives. To the best of our knowledge, the interactions between DPDI or relative derivatives and DNA have not been reported yet. The studies on the interactions between this type of carbazole derivatives and DNA would broaden the understandings and applications of 3,6-carbazole dicationic analogues whether as DNA structural probes or as cancer therapeutics targeted to DNA.

Herein, DPDI have been synthesized and characterized. Through multiple characterizations, the strong interactions with

View Article Online
DOI: 10.1039/C3OB40799C

DNA have been confirmed. However, whether –NH on DPDI participated in the interactions between DPDI and DNA was not clear. In order to clarify this and the interaction preferences of DPDI and DNA, another dicationic carbazole derivative, where a phenyl group was utilized to block –NH of carbazole group on DPDI, 2,8-Dimethyl-5-phenyl-5H-pyrrolo[3,2-c:4,5-c']dipyridinium diiodide (**DPPDI**, the structure is illustrated in Fig.1.), was synthesized and characterized. The spectral titrations of both DPDI and DPPDI with CT-DNA including UV-Vis absorption, fluorescence, and CD showed that both compounds had high affinities to DNA. The differences in CD titrations, Hoechst 33258 competitions and gel electrophoresis disclosed that DPDI interacted with DNA by mixing modes of intercalations and groove binding, while DPPDI displayed only groove binding mode. Moreover, both DPDI and DPPDI induced severe compression of DNA conformations, as demonstrated by atomic force microscopy (AFM).

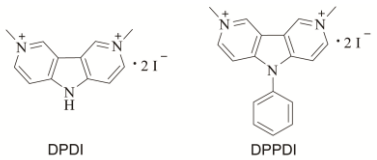

Fig. 1. The structures of DPDI and DPPDI.

Results and discussion

Fluorescence titration

DPDI has strong fluorescence at Ex/Em of 266 nm/ 388 nm and DPPDI has fluorescence at Ex/Em of 225 nm/ 395 nm. However, during the experiments, fluorescence decay over time was observed and it was different in aqueous solutions with various ionic strengths. Therefore, aqueous solutions with four various ionic strengths (10^{-4} M, 10^{-3} M, 10^{-2} M and 10^{-1} M) were tested to study the fluorescence intensity changing over time as exhibited in supplementary information Fig. S1. After 3 hours at room temperature, fluorescence of both DPDI and DPPDI decayed slowly. Therefore, DPDI or DPPDI solutions were placed at room temperature for 3 h before fluorescence titration.

Fluorescence titration by CT-DNA was applied to investigate the binding properties of DPDI/DPPDI with DNA. Fig. 2-1 and 2-2 illustrated the fluorescence changing of DPDI and DPPDI, respectively, by titration of CT-DNA at various ionic strengths.

At low ionic strength, the fluorescence of dicationic carbazoles was quenched quickly by DNA. Especially at low ionic strength of 10^{-4} M, dicationic carbazoles upon binding to DNA exhibited a maximal quenching of about 67% for DPDI and about 63% for DPPDI. With ionic strength increasing, fluorescence quenching was lessening gradually. For DPDI, at ionic strength of 10^{-1} M, fluorescence emission intensity increased at the earlier addition of DNA, then decreased when further addition of DNA. While for DPPDI at ionic strength of 10^{-2} M, the decrease of fluorescence after addition of DNA was negligible (less than 10%), and then there was no further experiments at ionic strength of 10^{-1} M.

Fluorescence changing (increasing or decreasing) is a criterion for the interactions between small molecules and DNA, and the extent of fluorescence quenching is corresponding to the strength of interactions. [20] At low ionic strength, the fluorescence of both dicationic carbazoles was greatly quenched by DNA, which indicated strong interactions between dicationic carbazoles and DNA. The interactions were weakening with ionic strength increasing.

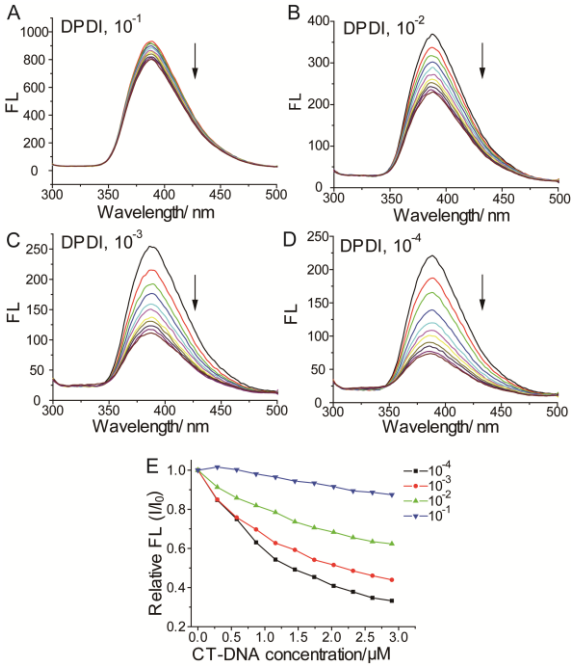

Fig.2-1. Fluorescence emission changes when titration of DPDI by CT-DNA. [DPDI] =0.1 μM in buffer of pH=7.4 (10^{-4} M Tris-HCl buffer); [DNA base pairs] = 0, 0.29, 0.58, 0.87, 1.16, 1.45, 1.74, 2.03, 2.32, 2.61, 2.90 μM. (A) ionic strength of 10^{-1} M; (B) ionic strength of 10^{-2} M; (C) ionic strength of 10^{-3} M; (D) ionic strength of 10^{-4} M; E. Relative fluorescence intensity decrease when titration of DPDI (0.1 μM) by CT-DNA (0-2.90 μM). Black line and squares: ionic strength of 10^{-4} M; Red line and diamonds: ionic strength of 10^{-3} M; Green line and triangles: ionic strength of 10^{-2} M; Blue line and inverted triangles: ionic strength of 10^{-1} M.

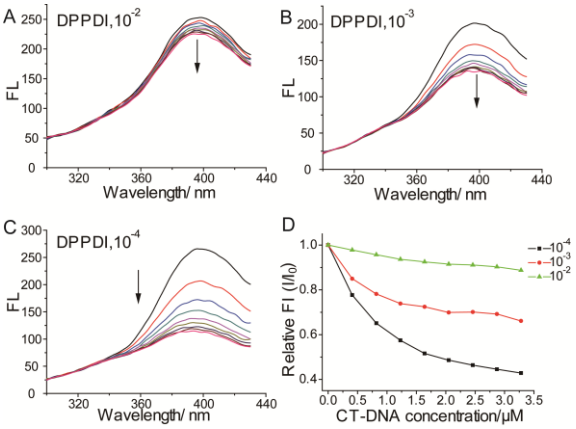

Fig. 2-2. Fluorescence emission changes when titration of DPPDI by CT-DNA. [DPPDI] =0.1 μM in buffer of pH=7.4 (10^{-4} M Tris-HCl buffer); [DNA base pairs] = 0, 0.41, 0.82, 1.23, 1.64, 2.05, 2.46, 2.87, 3.28 μM. (A) ionic strength of 10^{-2} M; (B) ionic strength of 10^{-3} M; (C) ionic strength of 10^{-4} M; (D) Relative fluorescence intensity decrease when titration of DPPDI (0.1 μM) by CT-DNA (0-3.28 μM). Black line and squares: ionic strength of 10^{-4} M; Red line and diamonds: ionic strength of 10^{-3} M; Green line and triangles: ionic strength of 10^{-2} M.

UV-Vis absorption titration

The absorption spectroscopy is the most common approach to investigate the interaction characteristics of small molecules with DNA. Red shift and hypochromism would happen in absorption spectrum of small molecules upon interacting with DNA. [21] It was generally accepted that the extent of the hypochromism in absorption spectrum was consistent with the strength of the interactions. [22]

View Article Online
DOI: 10.1039/C3OB40799C

Because the solubility of DPPDI was not good in aqueous solutions, DMSO was used as a solvent for preparing stock solution, but DMSO disturbed UV-Vis detection to some extent. Therefore, DNA binding properties of DPDI not DPPDI were studied by UV-Vis titration. Both DNA and DPDI have strong UV-Vis absorption, so there were two sets of UV-Vis titration experiments performed. The absorption spectra of DPDI titrated by CT-DNA were illustrated in Fig. 3-1 and UV-Vis titrations of CT-DNA titrated by DPDI were exhibited in Fig. 3-2. For the first set experiment, a reference cuvette contained corresponding CT-DNA alone to nullify the negative control absorbance. At low ionic strength of 10^{-4} M, titrations of CT-DNA into DPDI caused spectral changes obviously. Two major absorption peaks (270 and 330 nm) of DPDI exhibited apparent hypochromicity, with the maxima of 73.7% at 270 nm and 75.0% at 330 nm. However, another absorption peak of 226 nm exhibited no hypochromicity, but a small red shift of 2 nm. With ionic strength increasing, hypochromic effect decreased gradually and disappeared at 10^{-1} M. Furthermore, at low ionic strength of 10^{-4} M, clear isosbestic points were observed at 253 nm, 278 nm and 305 nm.

For the second set experiment, a reference cuvette contained corresponding DPDI alone to eliminate the negative control absorbance. At low ionic strength of 10^{-4} M, a distinct hypochromicity at 270 nm occurred. When ionic strength increased, hypochromic effect diminished regularly. It was indicative of considerable hypochromism in absorption spectrum of dicationic carbazole upon binding to DNA. These phenomena were consistent with the results obtained from Fig. 3-1. Additionally, blue shift from 260 to 251 nm of CT-DNA absorption peak was observed at ionic strength of 10^{-4} M, and a new absorption peak at 233 nm was also observed. It suggested the conformational changes of DNA in the presence of DPDI at low ionic strength.

The overall spectral changes with hypochromicity and isosbestic point induced by binding planar polyaromatic molecules to DNA are suggestive of strong interactions at low ionic strengths while weak interactions at high ionic strengths. [23]

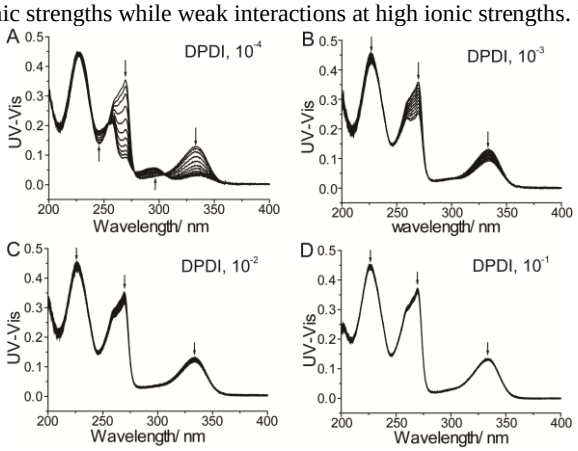

Fig.3-1 UV-vis absorbance changing with the titration of DPDI by CT-DNA. [DPDI] =10 μM in buffer of pH=7.4; [DNA base pairs] = 0, 3.88, 7.76, 11.64, 15.52, 19.40, 23.28, 27.16, 31.04, 34.92, 38.80 μM. (A) buffer (1.0×10^{-4} M Tris–HCl, 1.0×10^{-4} M NaCl); (B) buffer (1.0×10^{-3} M Tris–HCl, 1.0×10^{-3} M NaCl); (C) buffer (1.0×10^{-3} M Tris–HCl, 1.0×10^{-2} M NaCl); (D) buffer (1.0×10^{-3} M Tris–HCl, 1.0×10^{-1} M NaCl).

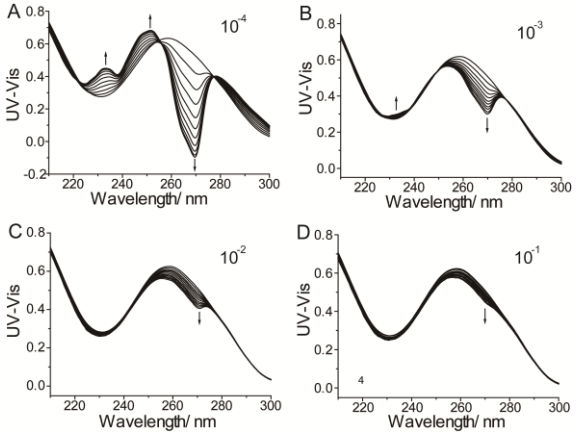

Fig. 3-2 UV-vis absorbance changing with the titration of CT-DNA by DPDI. [DNA base pairs] =48 μM in buffer of pH=7.4; [dicationic carbazole] = 0, 3.33, 6.67, 10.00, 13.33, 16.67, 20.00, 23.33, 26.67, 30.00, 33.33 μM. (A) buffer (1.0×10^{-4} M Tris–HCl, 1.0×10^{-4} M NaCl); (B) buffer (1.0×10^{-3} M Tris–HCl, 1.0×10^{-3} M NaCl); (C) buffer (1.0×10^{-3} M Tris–HCl, 1.0×10^{-2} M NaCl); (D) buffer (1.0×10^{-3} M Tris–HCl, 1.0×10^{-1} M NaCl).

Circular dichroism spectroscopy

Circular dichroism (CD) spectroscopy is a useful technique to analyze interactions between small molecules and DNA, and the observed changes of DNA CD signals are usually assigned to the corresponding changes in DNA structures. [24] Neither DPDI nor DPPDI has intrinsic CD signals due to achirality of the structures. Thus, the characteristic CD spectrum of CT-DNA in the region 220-320 nm could provide the information relevant to structural changes on DNA upon interactions with dicationic carbazoles. Fig. 4-1 and 4-2 depicted the CD spectra of CT-DNA with increasing concentrations of DPDI and DPPDI, respectively, at various ionic strengths.

The CD spectrum of free CT-DNA is of the typical B-form, with a positive Cotton effect near 275 nm due to base stacking and a negative Cotton effect near 245 nm due to right-handed helicity. [24] It is generally accepted that the classical intercalation enhances the base stacking and stabilizes helicity, and thus increases intensity of the positive band, whereas groove binding and electrostatic interaction of small molecules show less or no perturbation on the base stacking and helicity bands. [23]

For the CD spectra of DNA with the addition of DPDI, at ionic strength of 10^{-4} M as displayed in Fig. 4-1 D, there was a great enhancement for the positive band at 275 nm, which was probably due to intercalations of DPDI to DNA base pairs enhancing the base stacking. There was another positive band at 260-270nm observed much enhancement, which was not ascribed to intercalations. We deduced that it might be a result of groove interactions. The result was in conformity with our observation of UV-Vis titrations of CT-DNA by dicationic carbazole at low ionic strength of 10^{-4} M, and during UV-Vis titrations the blue shift from 260 to 251 nm of CT-DNA absorption peak and a new absorption peak of 233 nm were observed. At ionic strength of 10^{-3} M, the intensity of the positive band at 275 nm got doubled as shown in Fig. 4-1 C, while there was a little change for the band at 260-270 nm, which indicated that there were mainly the intercalative interactions between DPDI and CT-DNA at ionic strength of 10^{-3} M. With ionic strength increasing to 10^{-2} M, the intensity of the positive band at 275 nm increased with the maximum of 50.8%, which turned out the weakening of intercalative binding. At ionic strength of 10^{-1} M, the positive band at 275 nm showed little change, suggesting that high ionic strength could prevent the intercalative binding of DPDI to CT-

View Article Online
DOI: 10.1039/C3OB40799C

DNA. The intercalative binding of DPDI to CT-DNA at very low ionic strength made CT-DNA to be a shorter, more compact helical structure, which was consistent with the AFM results below.

For the CD spectra of DNA with DPPDI, at ionic strength of 10^{-4} M, there was almost no change for CD at 275nm as shown in Fig. 4-2 C, indicating that intercalative interactions do not exist between DPPDI and DNA, while there was a new positive band appeared at 260-270nm, which probably manifested the groove interactions between DPPDI and DNA at ionic strength of 10^{-4} M. With the increase of ionic strength, the groove interactions decreased. Because at ionic strength of 10^{-2} M, DPPDI had weak effect on CD of DNA, there were no further experiments for ionic strength of 10^{-1} M.

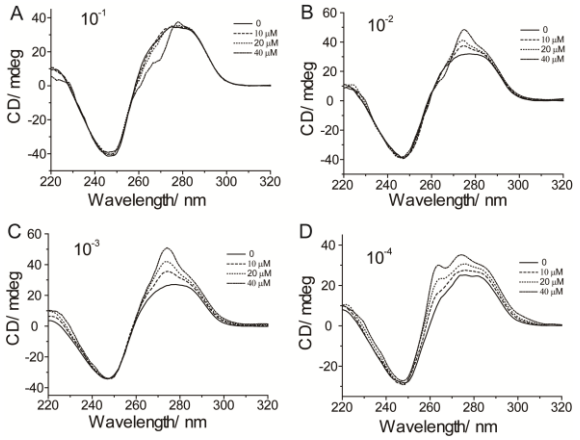

Fig. 4-1. CD spectra of CT-DNA (200 μM) at increasing DPDI concentration (0, 10, 20, 40 μM). (A) buffer (1.0×10^{-3} M Tris–HCl, 1.0×10^{-1} M NaCl); (B) buffer (1.0×10^{-3} M Tris–HCl, 1.0×10^{-2} M NaCl); (C) buffer (1.0×10^{-3} M Tris–HCl, 1.0×10^{-3} M NaCl); (D) buffer (1.0×10^{-4} M Tris–HCl, 1.0×10^{-4} M NaCl).

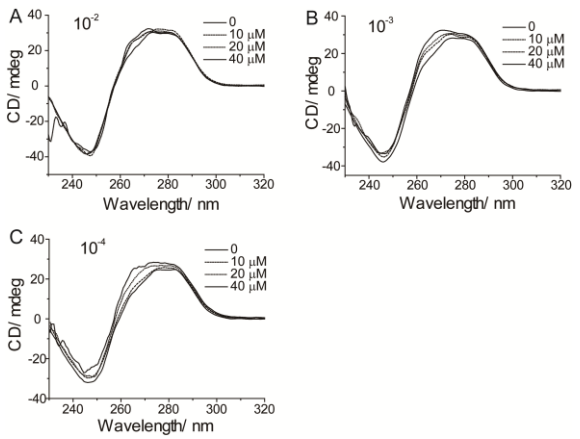

Fig. 4-2. CD spectra of CT-DNA (200 μM) at increasing DPPDI concentration (0, 10, 20, 40 μM). (A) buffer (1.0×10^{-3} M Tris–HCl, 1.0×10^{-2} M NaCl); (B) buffer (1.0×10^{-3} M Tris–HCl, 1.0×10^{-3} M NaCl); (C) buffer (1.0×10^{-4} M Tris–HCl, 1.0×10^{-4} M NaCl).

EB and H33258 competitive experiments

EB is a classical intercalator of DNA and H33258 is a representative DNA-groove binder. [25] To further confirm the interaction modes of the dicationic carbazoles with DNA, experiments of EB and H33258 competitive binding to DNA were carried out by the fluorescence spectra at two low ionic strengths (10^{-3} M and 10^{-4} M). Due to strong intercalative interactions between EB and DNA, DPDI or DPPDI was hard to replace EB from the complex of EB-DNA, so the EB competitive experiments revealed only relative small decrease of original fluorescence as shown in supplementary information Fig. S2. H33258 competitive results were shown in Fig. 5. The results revealed that the fluorescence of H33258 with DNA was decreasing rapidly with the addition of DPDI or DPPDI. 30 μM DPDI and DPPDI could quench the fluorescence for 45% and 46% at ionic strength of 10^{-4} M, respectively, and the fluorescence was quenched 26% and 39% at ionic strength of 10^{-3} M, respectively. The results indicated that both DPDI and DPPDI had strong groove interactions with DNA at ionic strength of 10^{-4} M, while at ionic strength of 10^{-3} M the groove interaction of DPPDI with DNA was stronger than DPDI. The conclusions accorded with the CD results of that at ionic strength of 10^{-4} M, the great enhancement of the positive band at 260-270 nm existed in the presence of either DPDI or DPPDI, while at ionic strength of 10^{-3} M CD revealed obvious enhancement at 260-270 in the presence of DPPDI, but little change in the presence of DPDI.

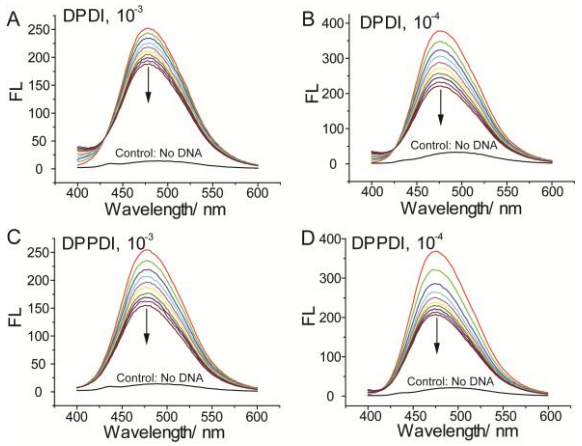

Fig. 5. Fluorescence spectra of H33258 (2 μM) and DNA (5 μM) with the increasing addition of DPDI ((A) ionic strength of 10^{-3} M and (B) ionic strength of 10^{-4} M) and DPPDI ((C) ionic strength of 10^{-3} M and (D) ionic strength of 10^{-4} M). [DPDI] or [DPPDI]= 0, 3.33, 6.67, 10.00, 13.33, 16.67, 20.00, 23.33, 26.67, 30.00 μM.

Gel electrophoresis

Gel electrophoresis is a general method to evaluate the binding mode of small molecules and DNA base pairs. [26, 27] Moreover, it was thought that intercalative interactions result in the band lag of the small molecule-DNA complex, while other binding modes do not affect the speed of band migration. [26] By DNA gel experiments, we tested the lpBR322 (linear pBR322) migration rate in the presence of DPDI or DPPDI at different ratios of dicationic carbazoles and DNA base pairs: 0, 1:1, 10:1 and 100:1 at low ionic strength of 10^{-4} M. The results were shown in Fig. 6A. Apparently, the band for high ratio of DPDI and base pairs was slower than low ratio, and especially at the ratio of 100:1, the band was much slower for DPDI, while for DPPDI, it seemed no change for all band positions. We also ran the gel experiments for the effects of EB and H33258 as shown in Fig. 6B. Obviously, EB made the lpBR322 band lagging but H33258 did not affect the rate of the band. The results indicated that DPDI, like EB, had obvious intercalative interactions with DNA at ionic strength of 10^{-4} M, while DPPDI, similar to H33258, mainly had groove binding with DNA at ionic strength of 10^{-4} M, which was consistent with CD and H33258 competitive results.

View Article Online
DOI: 10.1039/C3OB40799C

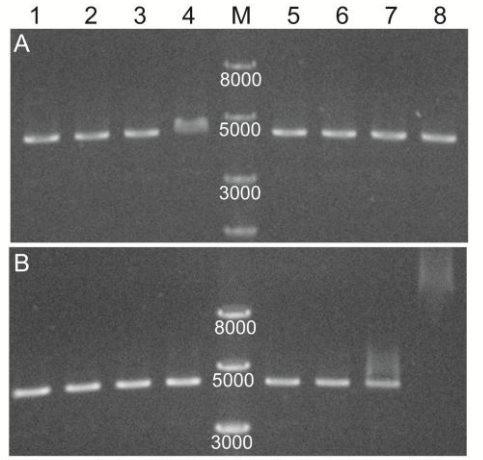

Fig. 6. (A) Gel electrophoresis of DNA (lpBR322) in the presence of increasing amount of DPDI (Lane 1-4) or DPPDI (Lane 5-8). (B) EB and H33258 acted as controls for classic intercalative interaction and groove interaction. M is marker.

AFM imaging

AFM experiments were carried out to manifest the DNA conformational changes induced by dicationic carbazoles at low ionic strength of about 10^{-3} M. Different dicationic carbazoles/pBR322 (bps) mixing ratios (0, 1:1, 10:1, 100:1) were adopted for the AFM studies. The images were shown in Fig. 7. With the increase of dicationic carbazoles/pBR322 ratios, the conformations of pBR322 were changed and presented compressing conformations, which was consistent with the results of CD spectra. The phenomena observed by AFM were similar to previously reported results [28], suggesting that both DPDI and DPPDI strongly interacted with DNA and induced pronounced changes in secondary structure of DNA at low ionic strength. However, AFM results cannot provide binding mode information, because either intercalation or groove binding can induce the conformational changes of DNA. [28, 29]

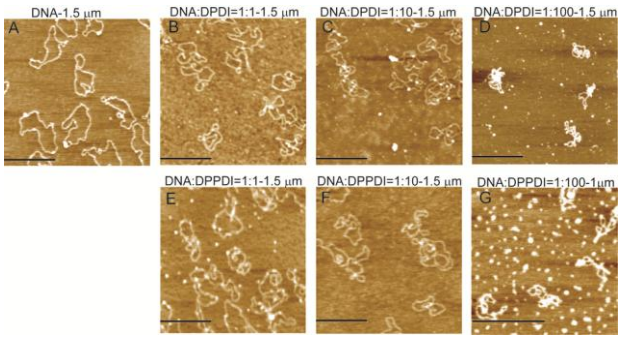

Fig. 7. AFM images for pBR322 with the increase of DPDI and DPPDI at the ratio of DNA:carbazole=1:0 (A), 1:1 ((B) and (E)), 10:1((C) and (F)), 100:1 ((D) and (G)). Scale bar: 500 nm.

DNA binding mode of dicationic carbazole-DNA

DPDI is a planar aromatic molecule, which contributes to the intercalation of DPDI to DNA base pairs. [2] The titrations of fluorescence and UV-Vis confirmed the strong interactions between DPDI and DNA, and also the obvious fluorescence decay of DPDI at low ionic strength was observed. Where did the fluorescence decay come from? Did it come from the production of $-N^-$ due to the dissociation of H from –NH of DPDI and thus aggregations due to the electrostatic interactions between $-N^-$ and cations of pyridinium at low ionic strength? In addition, it was worthy of exploring whether –NH participated to bind with DNA. It was reported that –NH groups of the carbazoles substituted at 2,7 positions with cationic amidine groups or imidazoline groups have been proved to bind strongly in the DNA groove of AT-rich sequences. [10, 11] Therefore, by introducing a phenyl group substituting H atom at –NH group of DPDI, DPPDI was designed to clarify the questions raised above. Moreover, the investigation of the interaction between DPPDI and DNA would settle another question: whether there were any other interaction modes existing between dicationic carbazole and DNA when benzene ring and carbazole ring of DPPDI were not in a plane, which would affect intercalation of dicationic carbazole to DNA.

Through theoretical calculations of 5-phenyl-5H-pyrrolo[3,2-c:4,5-c']dipyridine (2,8-dimethyl delection of DPPDI), the structure was similar to DPPDI, as shown in Fig. 8., which revealed that the angle between the plane of benzene ring and the plane of carbazole was 61.2°, so for DPPDI it was difficult to intercalate to DNA base pairs while there was other binding mode between DPPDI and DNA.

General DNA intercalators, such as EB, acridine orange and methylen blue, can intercalate with DNA at high ionic strength (10^{-1} M). [18] These DNA-intercalators have only one cation, while DPDI and DPPDI are dicationic compounds and the experimental results proved that ionic strength had great influence on the interactions between dicationic carbazoles and DNA. At high ionic strength, electrostatic interactions between ions in aqueous solutions and dications in carbazole promoted the solubility of carbazoles, increased the electronic density of the molecular plane and thus raised the fluorescence of the two carbazoles. However, at low ionic strength, the fluorescence of carbazole decayed greatly before stability, the reason of which was that an electrostatic balance of dications between carbazoles and a small amount of ions in aqueous solutions required time to reach and relative less electronic density to produce fluorescence.

At the mean time, ionic strengths had great effect on the interactions between carbazoles and DNA. At high ionic strength, strong electrostatic interactions diminished the interactions between carbazoles and DNA, while at low ionic strength, carbazoles displayed high binding affinity to DNA. In addition, through experiments for exploring or comparing the interactions between DPDI/DPPDI and DNA, the questions raised above got clear: the fluorescence decay did not come from the dissociation of –NH because DPPDI with block of –NH by phenyl group had the fluorescence decay at low ionic strength, and –NH of DPDI did not participate to groove binding with DNA because DPPDI had groove interaction with DNA. The phenyl ring and the carbazole ring of DPPDI was not in a plane, affecting DPPDI intercalating with DNA, while DPPDI still could bind with DNA through groove binding. The experimental results explained that DPDI could bind with DNA through mixing modes of intercalation and groove binding. Since both DPDI and DPPDI had groove binding with DNA, and the 3,6-carbazole compound binds in a more "classical" model that uses both cationic imidazoline or amidine groups for H-bonding while the carbazole NH points out of the groove [6, 7], similarly, when groove binding with DNA, dications of pyridinium on either DPDI or DPPDI can interact with DNA base pairs through groove binding, and –NH on DPDI or –N-Ph on DPPDI points out of the groove.

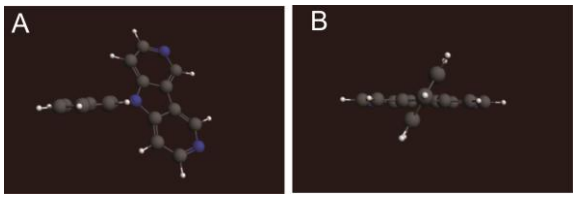

Fig. 8. Theoretical calculations on optimized molecular structure of 5-phenyl-5H-pyrrolo[3,2-c:4,5-c']dipyridine (2,8-dimethyl delection of DPPDI) were carried out at the DFT//B3LYP/6-31G level in the Amsterdam Density Functional (ADF) 2009.01 program.

Experimental Section

Synthesis

5-phenyl-5H-pyrrolo[3,2-c:4,5-c']dipyridine

A mixture of phenyl bromide (190 μL, 1.8 mmol), 5*H*-pyrrolo[3,2-c:4,5-c']dipyridine (100 mg, 0.59 mmol), CuI (12 mg, 0.06 mmol), 18-crown-6 (16 mg, 0.06 mmol), K_2CO_3 (165 mg, 1.2 mmol), and DMPU (1.0 mL) was stirred and heated to 190 ^oC in a sealed tube for 72 h. After cooling, the mixture was extracted with CH_2Cl_2, and the organic layer was dried over anhydrous Na_2SO_4. After removal of the solvent, the residue was purified by column chromatography on silica gel using CH_2Cl_2/MeOH (20:1, V:V) as the eluent to give a white powder, Yield: 66 %. ^1H NMR (DMSO-d_6) δ: 7.41 (d, J = 5.6 Hz, 2H, H_1, H_8), 7.60-7.74 (m, 5H, H_{ph}), 8.57 (d, J = 4.7 Hz, 2H, H_2, H_7), 9.58 (s, 2H, H_4, H_5); ^{13}C NMR (DMSO-d_6) δ: 106.01, 118.35, 126.92, 129.30, 130.89, 135.30, 144.06, 144.88, 146.94; IR (KBr) v: 3035, 2923, 1644, 1623, 1595 (C=C, C=N), 1502, 1470, 1384, 1232, 1192, 1166, 821, 757, 698 cm^{-1}; HRMS (ESI) *m/z* calcd for $C_{16}H_{12}N_3$ $[M+H]^+$ 246.1031, found 246.1023.

2,8-Dimethyl-5H-pyrrolo[3,2-c:4,5-c']dipyridinium diiodide (DPDI)

Methylation of 5*H*-pyrrolo[3,2-c:4,5-c']dipyridine by an excess amount of methyl iodide in MeOH afforded a yellow powder. ^1H NMR (DMSO-d_6) δ: 4.52 (s, 6H, CH_3), 8.41 (d, J = 7.0 Hz, 2H, H_1, H_8), 9.02 (d, J = 7.0 Hz, 2H, H_2, H_7), 10.03 (s, 2H, H_4, H_5); ^{13}C NMR (DMSO-d_6) δ: 48.34, 111.85, 118.82, 142.11, 143.48, 149.08; IR (KBr) v: 2936, 2786, 2637 (N-H), 1630, 1593 (C=C, C=N), 1472, 1271, 1246, 1183, 830 cm^{-1}; MS (ESI) *m/z*: 452 $[M-H]^-$; Anal. calcd for $C_{12}H_{13}I_2N_3$: C 31.81, H 2.89, N 9.27; found C 31.90, H 2.90, N 9.29.

2,8-Dimethyl-5-phenyl-5H-pyrrolo[3,2-c:4,5-c']dipyridinium diiodide (DPPDI)

Methylation of 5-pheny-5*H*-pyrrolo[3,2-c:4,5-c']dipyridine by an excess amount of methyl iodide in MeOH afforded a brown powder. ^1H NMR (DMSO-d_6) δ: 4.56 (s, 6H, CH_3), 7.77-7.88 (m, 5H, H_{ph}), 8.21 (d, J = 7.0 Hz, 2H, H_1, H_8), 9.06 (d, J = 7.1 Hz, 2H, H_2, H_7), 10.14 (s, 2H, H_4, H_5); ^{13}C NMR (DMSO-d_6) δ: 48.04, 110.14, 118.27, 126.86, 130.91, 132.28, 141.76, 144.02, 148.95; IR (KBr) v: 3014, 1668, 1633(C=C, C=N), 1590, 1500, 1471, 1337, 1258, 1186, 811, 770, 701 cm^{-1}; HRMS (ESI) *m/z* calcd for $C_{18}H_{17}IN_3$ $[M-I]^+$ 402.0467, found 402.0464.

5*H*-Pyrrolo[3,2-c:4,5-c']dipyridine was prepared as described previously. [19] The NMR spectrum was recorded on Bruker AV400 spectrometer. Infrared spectrum was obtained on a Thermo Nexus 470 spectrometer. Low resolution electrospray ionization (ESI) mass spectrum was obtained on AB SCIEX API4000 LC/MS. High resolution electrospray ionization (ESI) mass spectra were obtained on Thermo LTQ-Obitrap XL. Elemental analysis was performed on VarioEL III. The synthesis for the two dicationic carbazoles was outlined in Fig. S3 of supplementary information. The characteristic data of 5-phenyl-5H-pyrrolo[3,2-c:4,5-c']dipyridine, DPDI and DPPDI have been shown in the part of spectroscopic data in supplementary information.

Materials

Calf thymus DNA (CT-DNA), Ethidium Bromide (EB) and Hoechst 33258 was purchased from Sigma-Aldrich. Plasmid pBR322 were purchased from Toyobo Biochemicals. Reagents for synthesis were of chemical grade from Sinopharm Chemical Reagent Co, Ltd. Other reagents were of analytical grade from Sinopharm Chemical Reagent Co,Ltd unless specified otherwise. Double distilled deionized water was used to prepare buffers, and ionic strength in buffers was adjusted with NaCl. The CT-DNA concentration in base pairs was determined by an extinction coefficient of 1.32×10^4 M^{-1} cm^{-1} at 260 nm. The ratio A_{260}/A_{280} > 1.80 was used to indicate the high DNA purity. The DNA solution was stored for a short period of time at 4 ^oC if not used immediately. A DPDI stock solution (2×10^{-3} M) was prepared by dissolving an appropriate amount of DPDI in deionized water, and a DPPDI stock solution (2×10^{-3} M) was in deionized water/DMSO (1:1).

Fluorescence experiments

Fluorescence spectra and titrations were measured on a Perkin-Elmer LS-55 spectrometer (Perkin–Elmer Co., USA) with Ex/Em slit 10 nm/10 nm. Fluorescence decay was performed at a freshly diluted dicationic carbazoles (0.1 μM) in aqueous solutions with various ionic strengths. Fluorescence titrations were performed at a fixed dicationic carbazole concentration with various concentrations of CT-DNA. The fluorescence from 300 to 500 nm was recorded with Ex of 266 nm for DPDI, and fluorescence from 300 to 440 nm was recorded with Ex 225 for DPPDI.

UV-Vis absorption spectra

UV-Vis absorption spectra and titrations were recorded on a Perkin-Elmer Lambda 35 UV-Vis spectrometer (Perkin–Elmer Co., USA). The spectrometric measurements were performed at room temperature in a quartz cuvette of 1 cm path length, and the sample solution was stirred for 3 min before measurement. UV-Vis absorption titration experiments were performed at a fixed dicationic carbazole concentration (10 μM) in buffers with various ionic strengths and different CT-DNA concentrations (0-38.8 μM). A reference cuvette contained corresponding concentration of CT-DNA alone to nullify the absorbance of CT-DNA. Absorption titrations were performed at a fixed CT-DNA concentration (48 μM) in buffers of various ionic strengths with various concentrations (0-33.3 μM) of dicationic carbazole, and a reference cuvette contained corresponding concentrations of dicationic carbazoles alone to nullify the absorbance of dicationic carbazole.

Circular Dichroism

CD spectra were recorded on a Jasco J-810 spectrometer (Tokyo, Japan). The CD spectra of CT-DNA (200 μM) in buffers with various ionic strengths and different concentrations (0-40 μM) of DPDI and DPPDI were measured using a 1 cm path length cylindrical cell in the 220-320 nm wavelength region at room temperature. The bandwidth was 1 nm, and the response time was 1 s. Each spectrum is an average of two different scans obtained

View Article Online
DOI: 10.1039/C3OB40799C

by collecting data at 0.5 nm intervals with a scan speed of 200 nm/min.

H33258/EB competitive experiments

CT-DNA solutions with H33258 in different buffers were titrated by dicationic carbazoles of increasing concentration (0-30 μM), with the constant concentrations of CT-DNA (5 μM) and H33258 (2 μM). After each addition of dicationic carbazoles, the fluorescent emission spectra of H33258 from 400 to 600 nm were recorded with Ex of 380 nm on a Perkin-Elmer LS-55 spectrometer with Ex/Em slit 10 nm/5 nm.

A CT-DNA solution with EB (CT-DNA/EB 5 μM : 2 μM) in different buffer was prepared. The titration was performed similar to H33258 competitive experiments, where the fluorescent emission spectra of EB from 550 to 650 nm were recorded with Ex of 510 nm with Ex/Em slit 10 nm/10 nm.

Gel electraphoresis

The lpBR322 (linear pBR322) was obtained by the cleavage of pBR322 with BamHI (New England Biolabs, USA). The mixing ratios of dicationic carbazoles/EB/H33258 and pBR322 base pairs were 0, 1:1, 10:1 and 100:1. Electrophoresis was conducted at 120 V for 30~40 min in Tris/borate/EDTA buffer solution using 1% agarose gels to analyze DNA. The gel was stained with EB and photographed using UV illumination.

AFM experiments

The mixing ratios of dicationic carbazoles and pBR322 base pairs were 0, 1:1, 10:1 and 100:1. AFM experiments were performed as follows: take an aliquot of 10 μl mixture of dicationic carbazole and pBR322 in 10^{-3} M $NiCl_2$ aqueous solution and deposit it on the newly cleaved mica surface directly. The deposited droplet was left on the mica surface for 3-5 min and unattached pBR322 was washed with MilliQ water. Gently the sample was dried under a stream of nitrogen. Finally, samples were scanned with tapping mode on a PicoScan 2500 PicoSPM II controller (Agilent, USA) with a silicon probe of k = 40 N/m and 300 kHz resonant frequency.

Conclusions

In this work, a novel type of DNA binders-DPDI and DPPDI were synthesized and characterized. The DNA binding mode of dicationic carbazoles was elucidated based on the studies. Our studies showed the interactions between dicationic carbazoles and DNA were sensitive to ionic strength. The dicationic carbazoles could strongly interact with DNA at low ionic strength, and high ionic strength could prevent the interactions due to electrostatic interaction of dicationic carbazoles in aqueous solutions. In addition, the interactions between DPDI and DNA were demonstrated to be mixing interactions of intercalative binding and groove binding, while the interaction between DPPDI and DNA was mainly the groove interactions. The different interaction preferences of DPDI and DPPDI with DNA were decided by the similarity and difference in the structures between DPDI and DPPDI. Planar and aromatic DPDI had a strongly intercalative interaction with DNA, while in DPPDI, a phenyl group substituting H atom at –NH of DPDI destroyed molecular planarity, which resulted in no intercalative interactions. Both DPDI and DPPDI, belonging to 3,6-dicationic carbazoles, were similar to the classical model of DNA groove binding agents with an extended crescent shape. In groove interaction, dications of 3,6-dipyridinium on either DPDI or DPPDI interacted with DNA base pairs to closely fit the helical twist of the groove, and –NH on DPDI or –N-Ph on DPPDI pointed out of the groove.

Acknowledgements

The authors are grateful for the financial supports of National Natural Science Foundation of China (NO. 21002074, 21105114).

Notes and references

[a] *School of Pharmaceutical Sciences, Wuhan University, Wuhan, Hubei 430072, PR China Fax: +86-27-68759850, E-mail: jiat@whu.edu.cn*
[b] *State Key Laboratory of Virology, Wuhan Institute of Virology, Chinese Academy of Sciences, Wuhan, Hubei 430071, PR China Fax:+86-27-87199492, Email yujp@wh.iov.cn*

† Electronic Supplementary Information (ESI) available: Fluorescence decay, synthesis and characterization of DPDI and DPPDI were included. See DOI: 10.1039/b000000x/

‡ Footnotes should appear here. These might include comments relevant to but not central to the matter under discussion, limited experimental and spectral data, and crystallographic data.

1. A. Gluszynska, K. Bajor, I. Czerwinska, D. Kalet and B. Juskowiak, Tetrahedron Lett, 2010, 51, 5415-5418.
2. S. Catoen-Chackal, M. Facompre, R. Houssin, N. Pommery, J. F. Goossens, P. Colson, C. Bailly and J. P. Henichart, J Med Chem, 2004, 47, 3665-3673.
3. A. Manna and S. Chakravorti, J Phys Chem B, 2012, 116, 5226-5233.
4. D. Banerjee and S. K. Pal, J Phys Chem B, 2008, 112, 1016-1021.
5. N. N. Degtyareva, M. J. Fresia and J. T. Petty, Biochemistry-Us, 2007, 46, 15136-15143.
6. Y. Guan, R. Shi, X. M. Li, M. P. Zhao and Y. Z. Li, J Phys Chem B, 2007, 111, 7336-7344.
7. N. Dias, U. Jacquemard, B. Baldeyrou, C. Tardy, A. Lansiaux, P. Colson, F. Tanious, W. D. Wilson, S. Routier, J. Y. Merour and C. Bailly, Biochemistry-Us, 2004, 43, 15169-15178.
8. M. Munde, M. A. Ismail, R. Arafa, P. Peixoto, C. J. Collar, Y. Liu, L. X. Hu, M. H. David-Cordonnier, A. Lansiaux, C. Bailly, D. W. Boykin and W. D. Wilson, J Am Chem Soc, 2007, 129, 13732-13743.
9. L. X. Hu, Z. R. Li, Y. Li, J. R. Qu, Y. H. Ling, J. D. Jiang and D. W. Boykin, J Med Chem, 2006, 49, 6273-6282.
10. F. A. Tanious, D. Y. Ding, D. A. Patrick, C. Bailly, R. R. Tidwell and W. D. Wilson, Biochemistry-Us, 2000, 39, 12091-12101.
11. F. A. Tanious, D. Y. Ding, D. A. Patrick, R. R. Tidwell and W. D. Wilson, Biochemistry-Us, 1997, 36, 15315-15325.
12. F. A. Tanious, W. D. Wilson, D. A. Patrick, R. R. Tidwell, P. Colson, C. Houssier, C. Tardy and C. Bailly, Eur J Biochem, 2001, 268, 3455-3464.
13. X. J. Feng, P. L. Wu, F. Bolze, H. W. C. Leung, K. F. Li, N. K. Mak, D. W. J. Kwong, J. F. Nicoud, K. W. Cheah and M. S. Wong, Org Lett, 2010, 12, 2194-2197.
14. X. Liu, Y. M. Sun, Y. H. Zhang, F. Miao, G. C. Wang, H. S. Zhao, X. Q. Yu, H. Liu and W. Y. Wong, Org Biomol Chem, 2011, 9, 3615-3618.
15. Y. H. Zhang, J. J. Wang, P. F. Jia, X. Q. Yu, H. Liu, X. Liu, N. Zhao and B. B. Huang, Org Biomol Chem, 2010, 8, 4582-4588.
16. C. C. Chang, I. C. Kuo, J. J. Lin, Y. C. Lu, C. T. Chen, H. T. Back, P. J. Lou and T. C. Chang, Chem Biodivers, 2004, 1, 1377-1384.
17. F. C. Huang, C. C. Chang, P. J. Lou, I. C. Kuo, C. W. Chien, C. T. Chen, F. Y. Shieh, T. C. Chang and J. J. Lin, Mol Cancer Res, 2008, 6, 955-964.
18. X. F. Zhang, H. J. Zhang, J. F. Xiang, Q. A. Li, Q. F. Yang, Q. A. Shang, Y. X. Zhang and Y. L. Tang, J Mol Struct, 2010, 982, 133-138.
19. L. Kaczmarek, A. Becalski and P. Nantkanamirski, Pol J Chem, 1980, 54, 1585-1590.
20. T. Jia, Z. X. Jiang, K. Wang and Z. Y. Li, Biophys Chem, 2006, 119, 295-302.
21. Y. R. Kim, L. Gong, J. Park, Y. J. Jang, J. Kim and S. K. Kim, J Phys Chem B, 2012, 116, 2330-2337.
22. L. M. Chen, J. Liu, J. C. Chen, C. P. Tan, S. Shi, K. C. Zheng and L. N. Ji, J Inorg Biochem, 2008, 102, 330-341.
23. J. H. Tan, Y. J. Lu, Z. S. Huang, L. Q. Gu and H. Y. Wu, Eur J Med Chem, 2007, 42, 1169-1175.

View Article Online
DOI: 10.1039/C3OB40799C

24. V. I. Ivanov, Minchenk.Le, Schyolki.Ak and Poletaye.Ai, Biopolymers, 1973, 12, 89-110.
25. S. Y. Breusegem, R. M. Clegg and F. G. Loontiens, Journal of molecular biology, 2002, 315, 1049-1061.
26. R. J. Fiel and B. R. Munson, Nucleic Acids Res, 1980, 8, 2835-2842.
27. Q. G. Chen, D. H. Li, Y. Zhao, H. H. Yang, Q. Z. Zhu and J. G. Xu, Analyst, 1999, 124, 901-906.
28. K. Klemm, M. Radic Stojkovic, G. Horvat, V. Tomisic, I. Piantanida and C. Schmuck, Chemistry, 2012, 18, 1352-1363.
29. M. Saito, M. Kobayashi, S. I. Iwabuchi, Y. Morita, Y. Takamura and E. Tamiya, J Biochem, 2004, 136, 813-823.